JOURNAL OF SPACECRAFT AND ROCKETS
Vol. 45, No. 6, November–December 2008

Entry, Descent, and Landing Operations Analysis for the Stardust Entry Capsule

Prasun N. Desai*
NASA Langley Research Center, Hampton, Virginia 23681-2199
and
Dan T. Lyons,† Jeff Tooley,‡ and Julie Kangas§
Jet Propulsion Laboratory, California Institute of Technology, Pasadena, California 91109-8099

DOI: 10.2514/1.37090

On the morning of 15 January 2006, the Stardust capsule successfully landed at the Utah Test and Training Range in northwest Utah, returning cometary samples from the comet Wild-2. An overview of the entry, descent, and landing trajectory analysis that was performed for targeting during the mission operations phase upon final approach to Earth is described. The final orbit determination solution produced an inertial entry flight-path angle of −8.21 deg (the desired nominal value) with a 3-σ uncertainty of ±0.0017 deg (2% of the requirement). The navigation and entry, descent, and landing operations effort accurately delivered the entry capsule to the desired landing site. The final landing location was 8.1 km from the target, which was well within the allowable landing area. Overall, the Earth approach operation procedures worked well and there were no issues (logistically or performance-based) that arose. As a result, the process of targeting a capsule from an interplanetary trajectory and accurately landing it on Earth was successfully demonstrated.

I. Introduction

STARDUST, the fourth of NASA's Discovery-class missions, was launched on 7 February 1999. The spacecraft performed a close flyby of the comet Wild-2, coming within 149 km of the comet nucleus. The cometary samples were collected by extending a collection tray on a boom into the gas/dust freestream emanating from the comet (see Fig. 1), in which the particles were trapped in a material called aerogel. Once the collection process was completed, the collection tray was retracted back into the capsule. In addition to collecting cometary particles, Stardust also collected interstellar dust particles during its 7-year journey. Stardust was the first mission to return samples from a comet. Atkins et al. [1] provide an overview of the Stardust mission.

Upon Earth return on the morning of 15 January 2006, the entry capsule containing the cometary samples was released from the main spacecraft and descended through the Earth's atmosphere, decelerating with the aid of a parachute for a successful landing at the U.S. Air Force's Utah Test and Training Range (UTTR) in northwest Utah. Helfrich et al. [2] describe the Stardust Earth return trajectory strategy.

This paper provides an overview of the entry, descent, and landing (EDL) trajectory analysis that was performed for targeting the capsule to UTTR during the Stardust mission operations phase upon final approach to Earth. In addition, how the predicted landing location and the resulting overall 99% footprint ellipse (obtained from a Monte Carlo analysis) changed over the final days and hours before entry is also presented. This analysis was required to substantiate the robustness of the capsule descent to assure that all entry mission and public safety requirements were satisfied before gaining authorization for capsule separation from the main spacecraft for Earth entry.

II. Capsule Overview

The Stardust capsule (Fig. 2) is approximately 0.8 m in diameter. Its forebody is a blunted 60 deg half-angle sphere cone. The afterbody is a 30 deg truncated cone. The entry velocity for the Stardust capsule was the highest (inertial velocity of 12.9 km/s) of any Earth returning mission to date. For comparison, the Apollo lunar missions had entry velocities of 11.0 km/s. This high entry velocity resulted in the highest heating rates for any Earth returning vehicle. Traditional carbon-phenolic-based thermal protection systems are very effective at such intense heating levels; however, they are quite heavy. To remain within project mass limits, a new lightweight heat-shield material, phenolic impregnated carbon ablator, was used [3]. Willcockson [4] provides an overview of the Stardust capsule and its design.

III. Entry, Descent, and Landing Overview

Four hours before entry, the 45.8 kg capsule was spun up to 13.5 rpm and separated from the main spacecraft. The capsule had no active guidance or control systems, and so the spin-up was required to maintain its entry attitude (nominally 0 deg angle of attack) during coast. Figure 3 shows the nominal Stardust entry sequence with the terminal descent phases highlighted. Throughout the atmospheric entry, the passive capsule relied solely on aerodynamic stability for performing a controlled descent through all aerodynamic flight regimes: free molecular, hypersonic-transitional, hypersonic-continuum, supersonic, transonic, and subsonic. Therefore, the capsule was required to possess sufficient aerodynamic stability to minimize any angle-of-attack excursions during the severe heating environment. Additionally, this stability was needed throughout the transonic and subsonic regimes to maintain a controlled attitude at drogue and main parachute deployments. The nominal design values at entry interface (radius of 6503.14 km, equivalent to 125 km radial altitude) for the inertial entry velocity and inertial flight-path angle for the Stardust were 12.9 km/s and −8.2 deg, respectively.

Presented as Paper 6410 at the AIAA/AAS Astrodynamics Specialist Conference and Exhibit, Keystone, CO, 21–24 August 2006; received 11 February 2008; revision received 10 July 2008; accepted for publication 11 July 2008.

*Senior Engineer, Systems Engineering Directorate, 1 North Dryden Street, Mail Stop 489; prasun.n.desai@nasa.gov. Associate Fellow AIAA.

†Senior Engineer, Entry, Descent, and Landing, Aero Applications Group, 4800 Oak Grove Drive, Mail Stop 301-140L; daniel.t.lyons@jpl.nasa.gov. Member AIAA.

‡Engineer, Entry, Descent, and Landing, Aero Applications Group, 4800 Oak Grove Drive, Mail Stop 301-220G; jeffrey.tooley@jpl.nasa.gov.

§Engineer, Entry, Descent, and Landing, Aero Applications Group, 4800 Oak Grove Drive, Mail Stop 301-150; julie.a.kangas@jpl.nasa.gov.

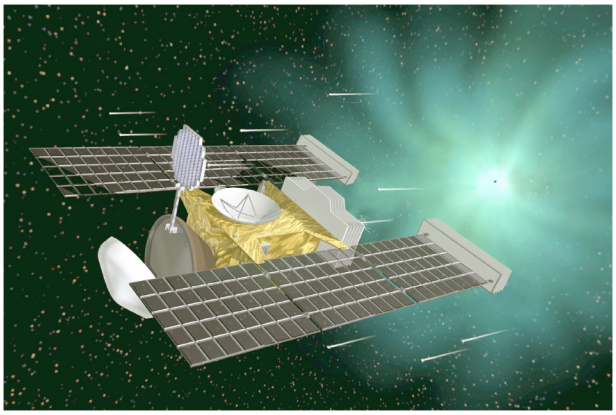

Fig. 1 Stardust spacecraft in sample configuration.

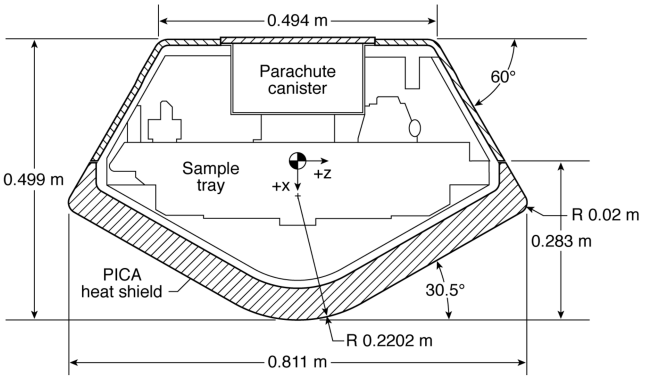

Fig. 2 Stardust capsule configuration (PICA denotes phenolic impregnated carbon ablator).

Desai et al. [5] provide an in-depth description on the development of the entry sequence: specifically, the use of the high spin rate and a supersonic drogue parachute. During descent, the capsule used a G-switch (i.e., gravity switch) and two timers for deployment of the drogue and main parachutes. The G-switch would be triggered after sensing a 3 *g* deceleration. At that point, the drogue timer is initiated. After 15.04 s, the drogue parachute is deployed at approximately Mach 1.37 (mean sea level altitude of 32 km), and the main timer is initiated. After 350.6 s [approximately Mach 0.16 and a mean sea level altitude of 3.1 km (1.8 km above ground)], the main parachute is deployed to slow the capsule for landing at UTTR. This nominal entry sequence was sufficiently robust to accommodate offnominal conditions during the descent, as shown by the Monte Carlo dispersion analyses described in [5].

IV. Earth Return Strategy

The Stardust event timeline for final Earth approach is shown in Fig. 4, which highlights the trajectory correction maneuvers (TCM) that were planned for attaining the proper entry conditions. Helfrich et al. [2] provide an overview of the Earth return strategy showing all of the required TCMs. Before TCM-18, which occurred at entry (E) minus 10 days, the Stardust return trajectory was on a path that missed the Earth. Only after TCM-18 was successfully executed did the trajectory of the spacecraft shift to be targeted within the Earth's atmosphere.

Final targeting was accomplished with TCM-19 at E–29 hours (h), which placed the nominal landing location in the eastern portion of UTTR. If TCM-19 had not executed or only partially executed, a contingency maneuver (TCM-19a or TCM-19b) would have been implemented at E–12 h to achieve the desired target landing location. At E–4 h, the capsule was separated from the main spacecraft, thus starting the EDL sequence illustrated in Fig. 3. The separation maneuver imparted to the capsule the remaining velocity increment required to target the desired nominal landing location at the center of UTTR. At E–3.7 h, a TCM was performed to divert the main spacecraft into an orbit ahead of the Earth. If TCM-18, 19, 19a, or 19b had all been unsuccessful, the capsule/main spacecraft would have flown by the Earth, as depicted in Fig. 4 by the solid line. During mission operations, both TCM-18 and TCM-19 executed very successfully, as did the separation and divert maneuvers. As a result, the desired entry conditions were achieved with very high accuracy [6].

V. Trajectory Simulation

A. Entry Trajectory Requirements and Constraints

The Stardust atmospheric-entry trajectory was designed to fit within an envelope of derived requirements and physical constraints based upon the capsule hardware design. As such, for a successful landing, all entry requirements must be satisfied. Table 1 lists all the EDL requirements and their specific bounds. Monte Carlo dispersion analyses, described in subsequent sections, were performed during the Earth approach mission operations phase to assess the satisfaction of these requirements.

B. Monte Carlo Uncertainty Sources

During the entry, offnominal conditions may arise that affect the descent profile. These offnominal conditions can originate from numerous sources: state vector uncertainties from orbit determination, capsule mass-property-measurement uncertainties; separation attitude and attitude rate uncertainties; limited knowledge of the entry day atmospheric properties (density and winds); uncertainty with the aerodynamics; and uncertainties with parachute deployment. In the analysis, an attempt was made to conservatively quantify

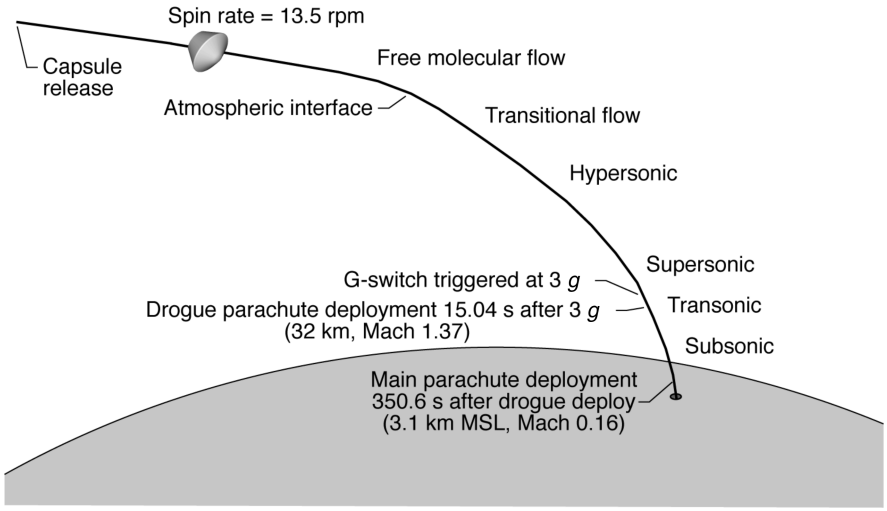

Fig. 3 Nominal Stardust capsule entry sequence (MSL denotes mean sea level).

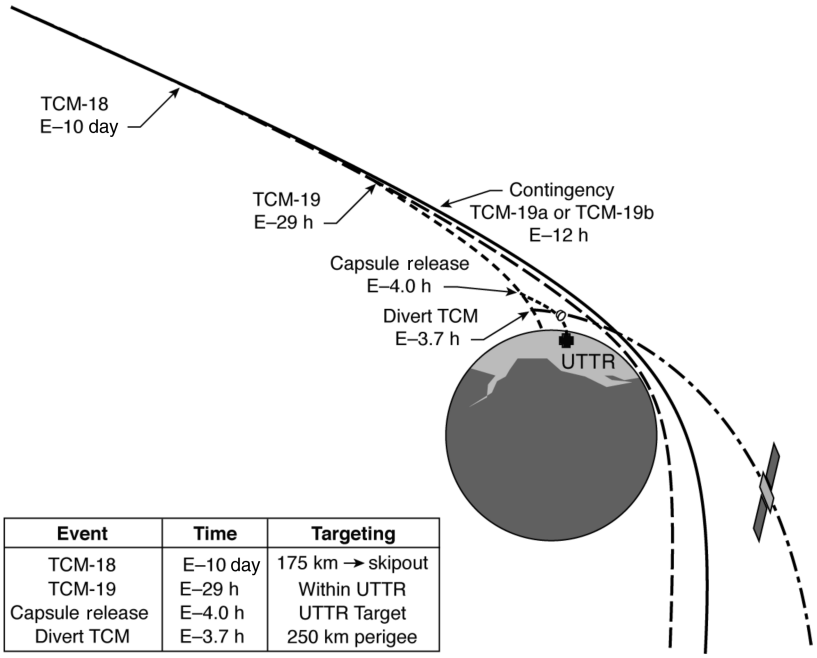

Event	Time	Targeting
TCM-18	E–10 day	175 km → skipout
TCM-19	E–29 h	Within UTTR
Capsule release	E–4.0 h	UTTR Target
Divert TCM	E–3.7 h	250 km perigee

Fig. 4 Stardust final Earth approach event timeline.

and model the degree of uncertainty in each mission parameter. For this entry, 41 potential uncertainties were identified [5]. Table 2 captures these uncertainty sources, along with their corresponding 3-σ variances. Desai et al. [5] provide an in-depth description of the analysis methodology developed and used during the Stardust capsule design phase and the quantification of the various uncertainty sources. The subsequent subsections describe in greater detail a few of the key uncertainty sources that were updated during the Earth approach mission operations phase before the entry as more knowledge was gained.

Table 1 EDL requirements and constraints

Requirement	Limit
Entry flight-path-angle error, deg	$< \pm 0.08$
Entry attitude, deg	<10
Maximum heat rate, W/cm^2	<1200
Attitude at maximum heat rate, deg	<10
Maximum heat load, KJ/cm^2	<32.0
Maximum deceleration, Earth gravity	<40
Drogue chute deployment attitude, deg	<30
Drogue chute deployment Mach number M	$1.2 < M < 1.6$
Landed footprint, km	<84

1. Entry Covariance

The Stardust strategy for Earth approach was designed to maximize public safety in light of possible anomalies and contingencies, while still preserving the capability to meet the entry requirements. As a result, a series of maneuvers were performed to set up the approach and entry (see [2]). Initial conditions at entry were obtained from orbit determination (OD) solutions performed by the Stardust Navigation Team. References [2,6,7] provide a description of the navigation process during the return phase and the determination of the final arrival conditions before entry. The navigation accuracy obtained for Stardust yielded extremely small state errors upon Earth arrival. The final orbit determination solution produced a nominal inertial entry flight-path angle of -8.21 deg with a 3-σ error of ± 0.0017 deg, which was well within the ± 0.08 deg requirement. The corresponding inertial velocity at entry interface was 12.799 km/s with a 3-σ error of only ± 0.003 m/s.

2. Capsule/Cruise-Stage Separation

Based on the final main spacecraft and capsule mass properties, a statistical separation analysis was performed to predict separation attitude and attitude rate errors. The attitude errors predicted in pitch and yaw were ± 0.56 deg in each axis. The attitude pitch and yaw rate errors were ± 2.83 deg /s in each axis, and the roll rate error was

Table 2 Monte Carlo analysis variables

Variable	3-σ variation	Distribution
Entry states	Based on OD covariance (see [6])	——
Radial center of mass offset, mm	± 0.254	Gaussian
Axial center of mass, mm	± 0.254	Gaussian
Moments of inertia (I_{xx}, I_{yy}, I_{zz}), kg · m^2	$\pm 2\%, \pm 5\%, \pm 5\%$	Gaussian
Cross products (I_{xy}, I_{xz}, I_{yz}),kg · m^2	$\pm 0.003, \pm 0.003, \pm 0.003$	Gaussian
Separation pitch and yaw attitude, deg	$\pm 0.56, \pm 0.56$	Gaussian
Separation pitch and yaw rates, deg /s	$\pm 2.83, \pm 2.83$	Uniform
Separation roll rate, deg /s	± 12.0	Gaussian
Aerodynamic coefficients	See [5]	——
Ablation mass loss	$\pm 10\%$	Gaussian
Drogue parachute drag coefficient	$\pm 10\%$	Uniform
Main parachute drag coefficient	$\pm 10\%$	Uniform
G-switch acceleration trigger value	$\pm 10\%$	Uniform
Drogue parachute timer, s	± 0.05	Uniform
Main parachute timer, s	± 0.05	Uniform
Atmosphere	GRAM-95 model (see [7])	——

±12.0 deg/s. These variations were used as inputs in the Monte Carlo analysis.

3. *Atmosphere Model*

The Earth atmosphere model used by Stardust for the entry trajectory design and analysis was the Global Reference Atmospheric Model, version 1995 (GRAM-95) [8]. This model is an amalgam of three empirically based global data sets of the Earth that can produce an atmosphere profile as a function of altitude for a given date, time, and positional location about the Earth. GRAM-95 produces a representative atmosphere, taking into account variations in diurnal, seasonal, and positional information for a given trajectory to produce nominal density, temperature, and pressure profiles and their statistical perturbations along the trajectory flight track. GRAM-95 is not a predictive model nor does it account for the possibility of potential weather fronts or storms, but rather provides a representative profile based on historical data for a given time, season, and location.

Figure 5 shows samples of a few randomly perturbed density profiles as a fraction of the nominal profile for the Stardust entry date of 15 January 2006 produced by the GRAM-95 model. Also depicted are the theoretical upper and lower (±3-σ) boundaries of the possible density variation. As seen, density variations between ±5 to ±25% are possible. In addition, GRAM-95 also produces nominal wind profiles and their statistical perturbations for the northward, eastward, and vertical wind components. Figures 6 and 7 show the nominal, as well as a few randomly sampled, wind profiles (for the Stardust entry date of 15 January 2006) for the northward and eastward wind components, respectively, along with their theoretical upper and lower (±3-σ) boundaries. Note that the ±3-σ upper and lower boundaries for the density and winds in Figs. 5–7 are theoretical limits and not actual profiles. That is, the dispersion for a given profile would have to remain at either its upper or lower boundary continuously for every altitude point throughout the profile. For a realistic profile from GRAM-95, such a situation is not possible. At certain altitudes, the value for the density or the wind components for random profiles could approach the theoretical upper or lower boundary; however, it would not remain continuously at that boundary throughout the entire altitude band (see the random profiles in Figs. 5–7). In the Monte Carlo analysis, an atmosphere profile (density and wind components) was randomly generated for each case having the characteristics shown in Figs. 5–7. Also depicted in Figs. 6 and 7 is the actual wind profile measured from a balloon 2 h before entry (E–2 h) of the winter blizzard that occurred over UTTR during entry, which will be discussed in a subsequent section.

C. Trajectory Analysis

Two trajectory propagation codes were used for the Stardust landing dispersion analyses: the Program to Optimize Simulated Trajectories (POST) [9] and the Atmospheric-Entry Powered Landing (AEPL) program [10]. Two codes were employed to obtain independent verification that the predicted nominal landing location and the overall size of the dispersed landing footprint ellipse were within the UTTR boundaries to ensure public safety.

The POST trajectory analysis was performed modeling six-degree-of-freedom (6DOF) dynamics, which included all forces and torques on the spacecraft, from entry interface to drogue parachute deployment. During this portion of the entry, the full set of capsule aerodynamics and mass properties was incorporated into the simulation to accurately model the hypersonic descent [5]. From drogue parachute deployment to landing, three-degree-of-freedom (3DOF) dynamics were used, in which only the drag force was modeled and was assumed to act opposite of the wind-relative velocity vector. The POST trajectory simulation seamlessly transitions from 6DOF to 3DOF dynamics within a single continuous simulation.

The version of the AEPL program used for Stardust employed 3DOF analyses throughout. Because the Stardust entry was unguided and uncontrolled, the 3DOF results from AEPL agreed well with the POST 6DOF/3DOF simulation. The POST results were selected as primary for the mission. In general, there was very good agreement between the two simulations.

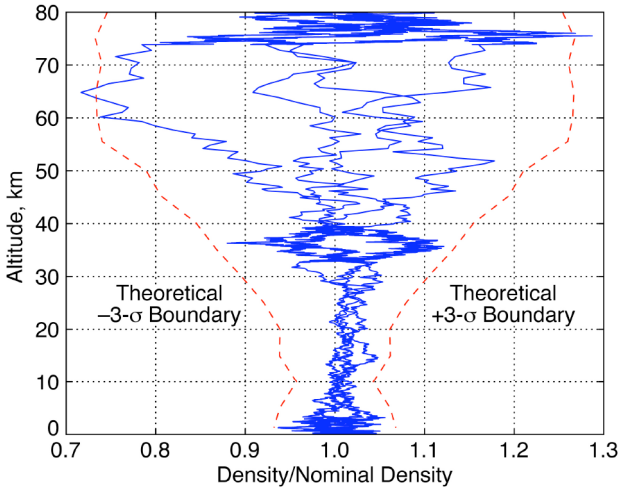

Fig. 5 Density variation from GRAM-95 model for 15 January 2006.

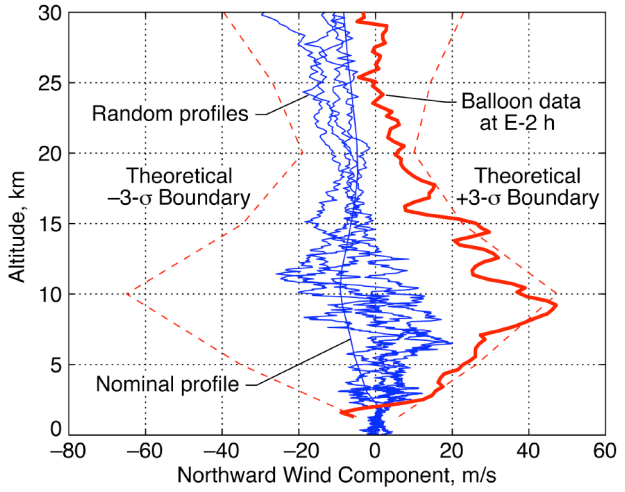

Fig. 6 Northward wind component variation from GRAM-95 model for 15 January 2006.

D. Entry Analysis Timeline

During Earth approach mission operations, entry analyses (described in the next section) had to be completed on a specific

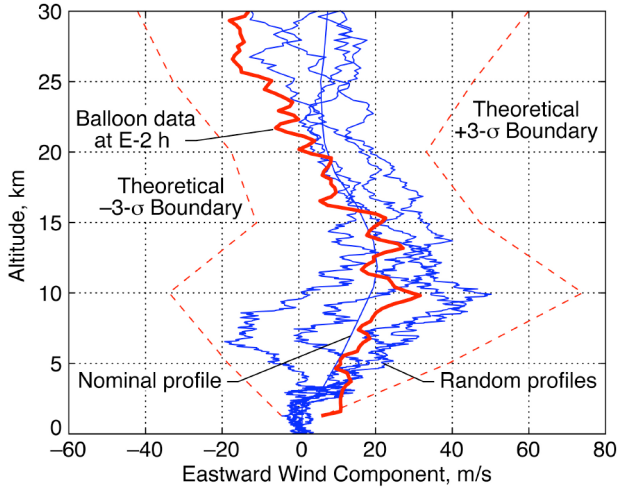

Fig. 7 Eastward wind component variation from GRAM-95 model for 15 January 2006.

timeline to allow decisions to be made regarding the Stardust landing. This Stardust timeline sequence builds on the experience gained during the Genesis Earth return mission operations effort performed in September 2004 [11,12]. The sequence of events before entry is listed in Table 3 (all times are relative to entry interface). TCM-19 at entry −29 h is listed as the first event, because it is the maneuver that targets Stardust to the desired landing location in the center of UTTR. Two go/no-go meetings (occurring at entry −21.5 h and entry −6.5 h) were held to review whether the EDL (see Table 1) and public safety (see [13]) requirements were satisfied. The go/no-go meetings were where the decisions were made to authorize Earth return. The go/no-go meetings 1 and 2 were the two most important times when the entry analyses results had to be available to assure that all EDL and public safety requirements were satisfied, because once the capsule was released from the main spacecraft at entry −4 h, there was nothing that could be done to modify the trajectory of the capsule. The entry results at both of these go/no-go meetings showed compliance of all requirements and led to decisions to authorize the entry. The go/no-go meeting 2 was the final opportunity to abort the entry if there were indications of any issues. The results showed compliance of all EDL and public safety requirements. Consequently, the entry sequence was allowed to continue for capsule release at entry −4 h from the main spacecraft and subsequent entry. The predicted landing location from the go/no-go meeting 2 results at entry −6.5 h was used to judiciously position the helicopter in UTTR to minimize the time for locating and retrieving a capsule after landing.

Leading up to the go/no-go meeting 1 and 2 decisions, the timeline was compressed. The entry, descent, and landing analyses (Monte Carlo and public safety) had to be performed within 90 min and compared with the requirements. A great amount of effort was spent practicing and streamlining this operation before these meetings. The 90 min were split, with 45 min allocated for the Monte Carlo dispersion analysis and 30 min for the public safety analysis (described in [13]), which required the Monte Carlo analysis results as input. The remaining 15 min were allocated for presentation material preparation. In general, 90 min was sufficient to complete the Monte Carlo dispersion and public safety analyses. Because the entry inertial fight-path angle attained was the desired nominal target of −8.21 deg with a 3-σ uncertainty of only ± 0.0017 deg (2% of the requirement), all the EDL and public safety metrics were well within their requirements and easily satisfied.

In general, a violation of any one of the EDL or public safety requirements at the go/no-go meetings would lead to a no-go decision for landing; however, in some cases, discretion was given to the project manager (at the entry −6.5 h meeting) as to whether the Stardust capsule would be authorized to separate from the main spacecraft. However, all events performed nominally, and there were no EDL or public-safety-requirement violations. The contingency maneuvers either TCM-19a or TCM-19b at entry −12 h were not required. Operationally, all the requirements were monitored weeks before the final approach and not just at these go/no-go meeting times. Overall, the Earth approach operation procedures worked well and there were no issues (logistically or performance-based) that arose.

E. Monte Carlo Dispersion Analysis

A Monte Carlo dispersion analysis was used during Earth approach mission operations to statistically assess the robustness of the Stardust entry to offnominal conditions to assure that all EDL requirements and constraints were satisfied (see Table 1). All the input parameters listed in Table 2 were randomly varied in the Monte Carlo dispersion analysis within their respective variances and distribution types. The analysis included uncertainties in the initial state vector, capsule mass properties (mass, center-of-gravity, and inertia), separation attitude and attitude rates, aerodynamic coefficients, ablation mass loss, atmospheric density and winds, parachute drag, G-switch trigger value, and parachute deployment timers.

For the dispersion analysis, 3000 random offnominal cases were run for all the navigation orbit determination (OD) solutions that were computed [6] at the various event times during the Earth approach mission operations phase. This analysis was performed to determine the appropriate magnitude and direction for the TCM-18 and TCM-19 maneuvers for proper targeting to UTTR. In addition, this analysis was used to assess the OD solution stability and to understand the movement of the nominal landing location and the variation in the 99% footprint-ellipse size within UTTR. This understanding was crucial to gain authorization for capsule separation and the subsequent Earth entry. The size of the 99% footprint ellipse obtained from the Monte Carlo dispersion analysis was used in a public safety probabilistic analysis to certify that the risks of the Stardust capsule entry were acceptable. Tooley et al. [13] describe the hazard analysis that was performed for the Stardust entry capsule using the 99% footprint ellipses generated by this Monte Carlo analysis. This hazard analysis was performed for the nominal scenario of an intact capsule, as well as for a burn-up and breakup scenario in case of capsule failure during the entry.

The Monte Carlo dispersion analysis was performed on all the post-TCM-18 OD solutions from OD s06008a through OD s06014a, where the first two numerical digits in the OD name refer to the year and next three numerical digits represent the day of the year that it was created (e.g., in OD 06014, 06 is 2006 and 014 represents the 14th day of the year). If there were multiple OD solutions on a given day, a letter extension was added to the end of the name (e.g., a, b, c, etc.). Figure 8 shows the corresponding results at landing, assuming that a perfect TCM-19 was executed. For clarity, only the results for three OD solutions are shown (OD s06011d, OD s06012b2, and OD s06014a), and their nominal landing locations (center points) and the 99% footprint ellipses at UTTR are depicted. The target location selected for Stardust was near the center of UTTR having the coordinates 246.55° east longitude and 40.3167° north latitude.

Over the course of the post-TCM-18 OD solutions, the nominal predicted landing location was observed to be stable with little drift. The nominal predicted landing locations are hard to differentiate, as they lie nearly on top of each other. The benefit of stable OD solutions is that greater confidence can be placed on the footprint size refinement. For the post-TCM-18 OD solutions, the 99% footprint ellipses decreased in size. The footprint size decreased from

Table 3 Timeline for entry

Time	Event
Entry −29 h	Execution of TCM-19
Entry −21.5 h	Go/no-go meeting 1
Entry −12 h	Execution of contingency TCM-19a or TCM-19b
Entry −6.5 h	Go/no-go meeting 2
Entry −4 h	Capsule release or divert
Entry +0	Entry interface

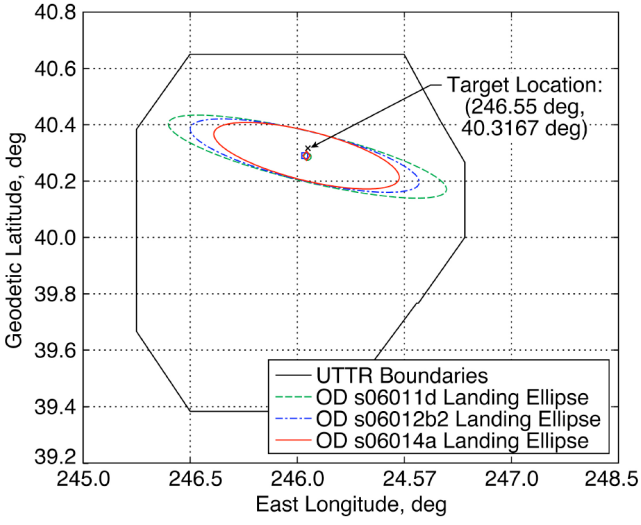

Fig. 8 Landing locations for post-TCM-18 OD solutions.

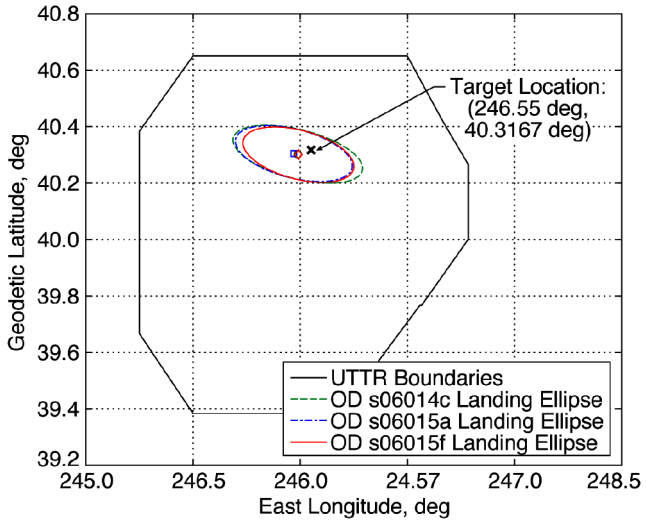

Fig. 9 Landing locations for post-TCM-19 OD solutions.

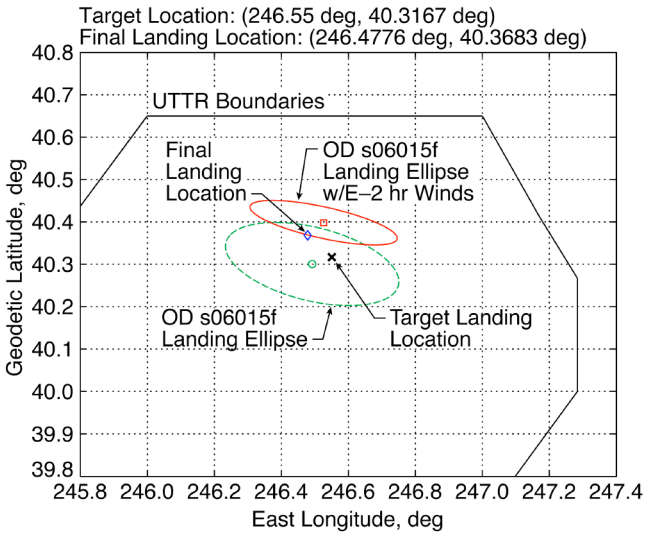

Fig. 10 Final capsule landing location.

113.3 km in downrange for OD s06011d to 75.5 km for OD s06014a. This reduction in footprint size arises from the increased OD observation time. Table 4 summarizes the variation in the 99% landed footprint-ellipse sizes. The corresponding inertial flight-path-angle errors at entry interface for these three OD solutions show a similar trend and are also summarized in Table 4.

Similarly, after TCM-19 was performed to move the landing location closer to the desired target, Monte Carlo analyses were performed for all the post-TCM-19 OD solutions (OD s06014b through OD s06014f). Figure 9 depicts the landing locations for a few of these OD solutions (OD s06014c, OD s06015a, and OD s06015f). All the OD solutions post-TCM-19 were extremely stable and produced nearly identical landing locations, as observed in Fig. 9, in which the 99% landing ellipses lie nearly on top of each other. The results for OD s06015f (which was the last OD solution available before entry) showed that all the EDL requirements and constraints were well within their limits and that the final predicted nominal landing location was very close to the desired target (only 5.7 km away). The footprint size for these OD solutions decreased from 52.7 km in downrange for OD s06014c to 45.1 km in downrange for OD s06015f. Table 4 summarizes the landed footprint variation, along with the variation in the corresponding inertial flight-path-angle error at entry interface. As seen, the inertial flight-path angle for OD s06015f was extremely small, with a value of only ± 0.0017 deg (2% of the requirement). As such, the navigation team accurately delivered the capsule to the desired entry conditions. Based on OD s06015f results of the predicted nominal landing location being 5.7 km away from the desired target and with a 99% footprint ellipse of 45.1 by 19.2 km, the authorization for capsule separation and subsequent Earth entry was granted.

Unfortunately, on entry day of 15 January 2006, a winter storm was moving through western Utah, which produced very strong winds over UTTR. The effect of strong winds would cause the capsule to drift from its predicted landing location during parachute descent. To address such a scenario, the Stardust entry operations strategy had planned two balloon launches to obtain measurements of the actual winds that were observed during the entry in an effort to better predict the landing location and footprint ellipse. These two balloon-measurement data revealed that very strong sustained winds were present over UTTR due to the winter blizzard. Figures 6 and 7 depict the actual wind profiles measured at E–2 h. As seen in Fig. 6, a very strong sustained wind to the north was present at E–2 h. This sustained northward wind component had a peak value of 50 m/s and corresponded to nearly the theoretical $+3\text{-}\sigma$ upper boundary throughout the altitude band. Because GRAM-95 does not account for the possibility of storms in its profiles, this sustained wind was well beyond the wind dispersions it produced and assumed in the Monte Carlo analysis. Consequently, an updated prediction of the nominal landing location (using this balloon-measured wind data) was performed to aid the retrieval of the capsule by notifying the recovery team of the change in landing location. This sustained northward wind pushed the capsule landing location toward the north, although the storm winds were predicted to subside over the remaining 2 h before landing.

Using this E–2 h balloon-measurement wind data, the Monte Carlo dispersion analysis was repeated with the GRAM-95 wind dispersions replaced with the E–2 h wind profile with no variations. Figure 10 shows the updated predicted nominal landing location and the 99% footprint ellipse. As seen, the OD s06015f landing prediction shifted north due to the E–2 h balloon-measurement wind data. The predicted nominal landing location moved from 5.7 km west–southwest of the target (circle) using the GRAM-95 wind profiles to 9.4 km north–northwest of the target (square). The updated 99% footprint ellipse was 38.1 by 8.2 km. The northward wind shifted the predicted nominal landing location approximately 11.5 km due north. The actual final landing location (diamond) is shown in Fig. 10 and was 8.1 km north–northwest of the desired target, which was within the OD s06015f preentry predicted 99% landing ellipse. Although the actual final landing location indicated that the capsule had not drifted as much to the north as the updated prediction, this outcome was likely caused by the winds

Table 4 Variation in landing footprint-ellipse size

OD solution	Event time	3-σ flight-path angle error, deg	99% footprint size, km
	Post-TCM-18		
s06011d	Entry −82 h	±0.144	113.3 × 19.7
s06012b2	Entry −41 h	±0.115	93.2 × 19.5
s06014a	Entry −32 h	±0.083	75.5 × 19.4
	Post-TCM-19		
s06014c	Entry −21 h	±0.033	52.7 × 19.3
s06015a	Entry −8 h	±0.021	47.5 × 19.2
s06015f	Entry −2 h	±0.0017	45.1 × 19.2
s06015f with E–2 h balloon data	Entry −2 h	±0.0017	38.1 × 8.2

subsiding (as forecasted) from that balloon-measured data at E–2 h, which was used in the updated prediction. Postflight reconstruction indicates that the actual Stardust entry was very close to the preentry predictions. Desai and Qualls [14] provide a detailed overview of the Stardust entry flight reconstruction and comparison to preentry predictions.

VI. Conclusions

On the morning of 15 January 2006, the Stardust entry capsule successfully descended through the Earth's atmosphere, decelerating with the aid of a parachute, and landed at the Utah Test and Training Range, completing a 7-year journey that returned cometary samples from the comet Wild-2. The final orbit determination solution produced an inertial entry flight-path angle of -8.21 deg (the desired nominal value) with a 3-σ error of ± 0.0017 deg (2% of the requirement). The navigation and the entry, descent, and landing trajectory analyses that were performed during the mission operations phase upon final approach to Earth accurately delivered the entry capsule to the desired landing site. The capsule landed 8.1 km from the desired target and was well within the allowable landing area at the Utah Test and Training Range. The entry, descent, and landing analyses had to be performed within a 90 min time frame to allow sufficient time for performing all the Earth approach procedures. All events performed nominally, and there were no entry requirement violations. Overall, the Earth approach operation procedures worked well and there were no issues (logistically or performance-based) that arose. As a result, the process of targeting a capsule from an interplanetary trajectory and accurately landing it on Earth was successfully demonstrated.

Acknowledgments

A portion of this research was carried out at the Jet Propulsion Laboratory, California Institute of Technology, under a contract with NASA. Reference herein to any specific commercial product, process, or service by trade name, trademark, manufacturer, or otherwise, does not constitute or imply its endorsement by the U.S. Government or the Jet Propulsion Laboratory, California Institute of Technology. The authors would like to acknowledge the efforts of the entire spacecraft operations, navigation, and entry, descent, and landing teams that resulted in such a successful mission.

References

[1] Atkins, K. L., Brownlee, D. E., Duxbury, T., Yen, C. W., Tsou, P., and Vollinga, J. M., "STARDUST: Discovery's InterStellar Dust and Cometary Sample Return Mission," *1997 IEEE Aerospace Conference*, Vol. 4, Inst. of Electrical and Electronics Engineers, Piscataway, NJ, Feb. 1997, pp. 229–245.

[2] Helfrich, C., Bhat, R., Kangas, J., Wilson, R., Wong, M., Potts, C., and Williams, K., "Maneuver Analysis and Targeting Strategy for the Stardust Re-Entry Capsule," AIAA Paper 2006-6406, Aug. 2006.

[3] Tran, H., Johnson, C., Rasky, D., Hui, F., Chen, Y.K., and Hsu, M., "Phenolic Impregnated Carbon Ablators (PICA) for Discovery Class Missions," AIAA Paper 96-1911, June 1996.

[4] Willcockson, W., "Stardust Sample Return Capsule Design Experience," *Journal of Spacecraft and Rockets*, Vol. 36, No. 3, May–June 1999, pp. 470–474. doi:10.2514/2.3468

[5] Desai, P. N., Mitcheltree, R. A., and Cheatwood, F.,M., "Entry Dispersion Analysis of the Stardust Sample Return Capsule," *Journal of Spacecraft and Rockets*, Vol. 36, No. 3, May–June 1999, pp. 463–469. doi:10.2514/2.3467

[6] Baird, D. T., Jah, Moriba., Jefferson, D., Kennedy, B., Lewis, G., Martin-Mur, T., McElrath, T., Mottinger, N., Nandi, S., and Thompson, P. F., "Stardust Earth Return Orbit Determination," American Astronautical Society Paper 07-429, Aug. 2007.

[7] Kennedy, B., Nandi, M., and McElrath, T., "Modeling of Deadband Delta-V for the Stardust Earth Return: Calibration, Analysis, Prediction, and Performance," AIAA Paper 2006-6408, Aug. 2006.

[8] Justus, C. G., Jeffries, W. R., III, Yung, S. P., and Johnson, D. L., "The NASA/MSFC Global Reference Atmospheric Model 1995 Version (GRAM-95)," NASA TM-4715, Aug. 1995.

[9] Brauer, G. L., Cornick, D. E., and Stevenson, R., "Capabilities and Applications of the Program to Optimize Simulated Trajectories (POST)," NASA CR-2770, Feb. 1977.

[10] Klumpp, A. R., *Atmospheric-Entry, Powered Landing Simulator V4.10C User's Guide*, Jet Propulsion Lab., California Inst. of Technology, Pasadena, CA, Apr. 2003.

[11] Desai, P. N., and Lyons, D. T., "Entry, Descent, and Landing Operations Analysis for the Genesis Entry Capsule," *Journal of Spacecraft and Rockets*, Vol. 45, No. 1, Sept.–Oct. 2008, pp. 27–32. doi:10.2514/1.30024

[12] Wawrzyniak, G., and Wahl, T., "Human Safety Analysis for the Genesis Sample Return Mission," American Astronautical Society Paper 05-223, Jan. 2005.

[13] Tooley, J., Desai, P. N., Lyons, D. T., Hirst, E., Wahl, T., Ivano, M., and Wawrzyniak, G., "Landing and Population Hazard Analysis for Stardust Entry in Operations and Entry Planning," AIAA Paper 2006-6412, Aug. 2006.

[14] Desai, P. N., and Qualls, G. D., "Stardust Entry Reconstruction," AIAA Paper 2008-1198, Jan. 2008.

C. Kluever
Associate Editor